2-15-2016

Differential Expression of Pancreatic Protein and Chemosensing Receptor mRNAs in NKCC1-null Intestine

Emily M. Bradford
University of Kentucky, emily.bradford@uky.edu

Kanimozhi Vairamani
University of Cincinnati

Gary E. Shull
University of Cincinnati

Differential Expression of Pancreatic Protein and Chemosensing Receptor mRNAs in NKCC1-null Intestine

Notes/Citation Information
Published in *World Journal of Gastrointestinal Pathophysiology,* v. 7, issue 1, p. 138-149.

Digital Object Identifier (DOI)
https://doi.org/10.4291/wjgp.v7.i1.138

World Journal of Gastrointestinal Pathophysiology

Submit a Manuscript: http://www.wjgnet.com/esps/
Help Desk: http://www.wjgnet.com/esps/helpdesk.aspx
DOI: 10.4291/wjgp.v7.i1.138

World J Gastrointest Pathophysiol 2016 February 15; 7(1): 138-149
ISSN 2150-5330 (online)

ORIGINAL ARTICLE

Basic Study

Differential expression of pancreatic protein and chemosensing receptor mRNAs in NKCC1-null intestine

Emily M Bradford, Kanimozhi Vairamani, Gary E Shull

Emily M Bradford, Department of Internal Medicine, Division of Gastroenterology, University of Kentucky, Lexington, KY 40536-0298, United States

Kanimozhi Vairamani, Gary E Shull, Department of Molecular Genetics, Biochemistry and Microbiology, University of Cincinnati College of Medicine, Cincinnati, OH 45267-0524, United States

Author contributions: Bradford EM and Shull GE conceived the study, analyzed the data, and wrote the manuscript; Vairamani K analyzed and compiled microarray data; Bradford EM performed all of the experiments.

Supported by National Institutes of Health to Gary E Shull, No. DK050594.

Institutional review board statement: Because human subjects or tissues were not used in this study, approval from the institutional review board was not required. Ethical issues relating to the animal protocol were reviewed and approved by the Institutional Animal Care and Use Committee of the University of Cincinnati.

Institutional animal care and use committee statement: All procedures involving animals were reviewed and approved by the Institutional Animal Care and Use Committee (IACUC) of the University of Cincinnati (protocol number: 06-06-22-02).

Conflict-of-interest statement: The authors have no conflict of interest related to this manuscript.

Data sharing statement: The microarray data have been deposited in the National Center for Biotechnology Gene Expression Omnibus and can be freely accessed as described in Methods. The Slc12a2 (NKCC1) knockout mouse model has been deposited in a publically available repository and can be accessed as described in Methods.

Correspondence to: Gary E Shull, PhD, Professor, Department of Molecular Genetics, Biochemistry and Microbiology, University of Cincinnati College of Medicine, 231 Albert Sabin Way, Cincinnati, OH 45267-0524, United States. shullge@ucmail.uc.edu
Telephone: +1-513-5580056
Fax: +1-513-5591885

Received: June 29, 2015
Peer-review started: July 2, 2015
First decision: September 22, 2015
Revised: October 10, 2015
Accepted: December 17, 2015
Article in press: December 18, 2015
Published online: February 15, 2016

Abstract

AIM: To investigate the intestinal functions of the NKCC1 Na^+-K^+-2Cl cotransporter (*SLC12a2* gene), differential mRNA expression changes in NKCC1-null intestine were analyzed.

METHODS: Microarray analysis of mRNA from intestines of adult wild-type mice and gene-targeted NKCC1-null mice (n = 6 of each genotype) was performed to identify patterns of differential gene expression changes. Differential expression patterns were further examined by Gene Ontology analysis using the online Gorilla program, and expression changes of selected genes were verified using northern blot analysis and quantitative real time-polymerase chain reaction. Histological staining and immunofluorescence were performed to identify cell types in which upregulated pancreatic digestive enzymes were expressed.

RESULTS: Genes typically associated with pancreatic function were upregulated. These included lipase, amylase, elastase, and serine proteases indicative of pancreatic exocrine function, as well as insulin and regenerating islet genes, representative of endocrine function. Northern blot analysis and immunohistochemistry showed that differential expression of exocrine pancreas mRNAs was specific to the duodenum and localized to a subset of goblet cells. In addition, a major pattern of changes involving differential expression of olfactory receptors that function in chemical sensing, as well as other chemosensing G-protein coupled receptors, was observed. These changes in chemosensory receptor expression may be related to the failure of intestinal function and dependency on parenteral nutrition observed in humans with *SLC12a2* mutations.

CONCLUSION: The results suggest that loss of NKCC1 affects not only secretion, but also goblet cell function and chemosensing of intestinal contents *via* G-protein coupled chemosensory receptors.

Key words: *SLC12a2*; Chemosensory; Chemosensitivity; Gastrointestinal; Dyspepsia

Core tip: The NKCC1 Na^+-K^+-$2Cl^-$ cotransporter is a major mechanism of Cl^- uptake in support of secretion. To investigate its intestinal functions we analyzed mRNA expression changes in NKCC1-null intestines. Differentially expressed genes included digestive enzymes and a large number of olfactory and other G-protein coupled receptors that function in chemical sensing. This suggests that loss of NKCC1 affects not only secretion, but also digestion and chemosensing of components of the intestinal contents. The results likely have relevance to recent evidence showing that mutations in the human *NKCC1* gene cause unexplained food intolerance and failure of intestinal function requiring parenteral nutrition.

Bradford EM, Vairamani K, Shull GE. Differential expression of pancreatic protein and chemosensing receptor mRNAs in NKCC1-null intestine. *World J Gastrointest Pathophysiol* 2016; 7(1): 138-149 Available from: URL: http://www.wjgnet.com/2150-5330/full/v7/i1/138.htm DOI: http://dx.doi.org/10.4291/wjgp.v7.i1.138

INTRODUCTION

The NKCC1 Na^+-K^+-$2Cl^-$ cotransporter, encoded by the *SLC12A2* gene, is expressed in all mammalian tissues and is particularly prominent in epithelial cells of the gastrointestinal tract[1]. Detailed immunohistochemical studies show that it is localized to basolateral membranes of intestinal secretory epithelia[1], where it mediates uptake of much of the Cl^- that is then secreted through the apical cystic fibrosis transmembrane conductance regulator (CFTR). In addition to secretory epithelia, NKCC1 is expressed in all segments of the gastrointestinal tract and throughout the crypt and villus epithelium, including both absorptive cells and goblet cells[1]. Thus, loss or inhibition of NKCC1 could have wide-ranging effects on gastrointestinal function. In fact, a National Institutes of Health web site (http://www.genome.gov/27551936) on Rare or Undiagnosed Diseases reports that humans with *SLC12A2* mutations have "exercise intolerance, dilated cardiomyopathy, and episodic hypoglycemia progressing to unexplained failure of intestinal function/food tolerance with subsequent parenteral nutrition dependency". The basis for the severe intestinal phenotype in humans is not known, but since it does not mimic the Cystic Fibrosis intestinal phenotype, it is unlikely to be due entirely to the secretory defect.

When anion secretion is impaired, the intestinal lumen can become desiccated, which leads to constipation, obstructions, and intussusception. Mice lacking CFTR usually develop lethal intestinal obstructions by 6 wk of age and require treatment with an osmotic laxative for normal survival[2], but the intestinal phenotype of *Nkcc1*$^{-/-}$ mice is much less severe[3]. In the original study, a small percentage of the *Nkcc1*$^{-/-}$ mice on a mixed genetic background developed intestinal impactions[3]. However, *Nkcc1*$^{-/-}$ mice on the FVB/N background (Swiss mice carrying the Fv1b sensitizing allele) that were used for the current study do not develop impactions, and the intestinal tract appears histologically normal.

Loss of NKCC1 in mice causes a defect in intestinal anion secretion as measured by reductions in the bumetanide-sensitive component in short circuit currents in duodenum, jejunum, and cecum[3-5]. However, compensatory pathways for basolateral Cl^- uptake have been identified in duodenum and colon[5,6], providing an explanation of why the loss of NKCC1 does not cause a profound defect in anion secretion in the intestinal tract. To gain a better understanding of the functions of NKCC1 and the molecular consequences of NKCC1-deficiency in the intestine, we performed microarray analyses of mRNA from *Nkcc1*$^{-/-}$ small intestine. The observed alterations in the expression of mRNAs encoding digestive enzymes and receptors that mediate chemical sensing could be involved in intestinal pathologies resulting from the inhibition or loss of NKCC1.

MATERIALS AND METHODS

NKCC1-null mutant mouse model

Nkcc1$^{-/-}$ mice were generated as previously described[3] and inbred onto the FVB/N background for at least 10 generations. FVB/N are Swiss mice, derived from the HFSF/N strain, which carry the Fv1b (Friend Leukemia Virus strain B) sensitizing allele. These *Nkcc1*$^{-/-}$ mice are available from the Jackson Labs Mutant Mouse Regional Resource Center and can be identified by searching

Table 1 Primer sequences used for quantitative real-time polymerase chain reaction and northern blot analyses

Name	Sequence
Pdx1	F: ACCAAAGCTCACGCGTGGAAA
	R: TGATGTGTCTCTCGGTCAAGTT
Insulin 1	F: TTGCCCTCTGGGAGCCCAAA
	R: CAGATGCTGGTGCAGCACTG
Insulin 2	F: TCTTCCTCTGGGAGTCCCAC
	R: CAGATGCTGGTGCAGCACTG
Glut2	F: CATTGCTGGAAGAAGCGTATCAG
	R: GAGACCTTCTGCTCAGTCGACG
Amylase	F: TTAACGATAATAAATGTAATGGAGAA
	R: CCCTGCTACTCCAATGTCAA
Trypsin	F: TGAGCAGTTTGTCAATTCTGCC
	R: GCATGATGTCGTTGTTCAGGG
Elastase	F: GTAGTTGCAGCCCAGAGAGG
	R: TCTGCTATGTCACAGGCTGG
Gp2	F: TCCCTGCCAGAATCACACGGT
	R: GGAGGTCCTGCCTACAGACACA
L32	F: GATCTAGCGGCCGCCATCTGTTTACGGCATCATG
	R: TAGATCGCGGCCGCCGCTCCCATAACCGATGTTGG

Forward and reverse primers for quantitative real-time polymerase chain reaction and northern blot probes are listed 5′ to 3′.

(http://www.jax.org/mmrrc/) with the gene symbol *Slc12a2* (strain name: FVB.Cg-Slc12a2tm1Ges). Wild-type (WT) FVB/N mice were originally obtained from Jackson Labs and bred in house. All experimental pairs were derived by breeding of NKCC1 heterozygous breeding pairs, were between 8 and 12 wk of age, and were age- and gender-matched. Mouse numbers (*n*) are indicated in methods or figure legends. Mice were maintained in a specific pathogen-free barrier facility, with access to food and water *ad libitum*, and all experiments were approved by the University of Cincinnati Animal Care and Use Committee.

Isolation of intestinal tissues

Mice were anesthetized by intraperitoneal injection of Avertin (2.5% solution of Tribromethanol) at 500 mg/kg, followed by cervical dislocation after the mice were anesthetized. Intestinal segments were removed and flushed with ice-cold phosphate-buffered saline. Some samples were frozen in liquid nitrogen and used for extraction of total RNA using Tri-Reagent (Molecular Research Center) and others were processed for immunolocalization studies as described in detail below.

Northern blot analysis and real-time polymerase chain reaction

Northern blot analysis was performed using 10 mg of total RNA per sample, and blots were hybridized with ^{32}P-labeled cDNA as previously described[7]. Primer sequences are given in Table 1. Quantification of band intensity, including background subtraction and normalization to the ribosomal L32 subunit mRNA, was done using ImageQuant software (Amersham Biosciences).

For quantitative real-time polymerase chain reaction (PCR), 4 μg of total RNA was reversed transcribed using oligo d(T) and SuperScript Ⅱ reverse transcriptase (Invitrogen). The cDNA was diluted 5-fold in water. Primer sequences are given in Table 1. For each primer set, optimization using serially-diluted standards and melting curve analysis was performed. Real-time PCR was run on a DNA Engine Opticon Ⅱ (MJ Research) thermalcycler using iQ SYBR Green (BioRad). For each gene, samples were run at least in duplicate, and mean values were normalized to the expression of *L32*. Standard curves were prepared for each gene on every run. All pairwise comparisons were done using a student's *t*-test; *P*-values of < 0.05 were considered significant.

Morphology and immunofluorescence

Intestinal segments were fixed in 10% neutral buffered formalin overnight and embedded in paraffin. Goblet cells were identified with hemotoxylin and eosin (H and E) or Alcian Blue/Periodic Acid-Schiff (AB/PAS) staining as described previously[8]. For immunofluorescence, sections ($n = 4$ WT and 3 NKCC1-null mutant) were deparaffinized in Citrisolve, rehydrated through successive ethanol washes, and boiled for 5 min in a sodium citrate buffer. Sections were incubated with primary antibodies for 12 h at room temperature, washed, and incubated with either another primary antibody or the appropriate secondary antibodies for 12 h at room temperature. Polyclonal antibodies against amylase (Sigma), trypsin (Abcam), elastase (Abcam), and intestinal trefoil factor 3 (TFF3) (ITF-Santa Cruz Biotechnology) were used at a 1:100 dilution; all secondary antibodies (Alexa Fluor, Molecular Probes) were used at a 1:200 dilution, and DAPI was included in the mounting medium (Vector Laboratories) for staining of nuclei. For localization studies using both fluorescence and AB/PAS, immunohistochemistry was done first and the slides were photographed. The slides were then washed, AB/PAS staining was performed, and the same areas were imaged. For colocalization studies, images were merged in Adobe Photoshop.

Microarray analysis

Microarray analyses were performed by the University of Cincinnati Genomics and Microarray Laboratory core facility exactly as described previously[8] using the Duke University Murine Operon v.3.0 spotted Array, which consisted of the Operon mouse oligonucleotide library, version 3.0, comprised of 70-mer oligonucleotides representing mouse genes. For analysis of NKCC1-null small intestine, total RNA was isolated from the entire small intestine of 8-wk old WT and NKCC1-null mutant (KO) mice ($n = 6$ of each genotype) on the FVB/N background, and cDNA was generated and labeled with Cy3 or Cy5 fluorophores and hybridized with the microarrays. The fold-changes and statistical significance for the microarray analysis were calculated exactly as described previously[8]. Briefly, Cy3 and Cy5 labeling

was alternated between WT and KO samples (dye-flip controls) to control for the influence of fluorophore labeling on probe hybridization. Values are represented as fold-changes (ratio of fluorescence intensity values), with positive values indicating upregulation and negative values indication downregulation in KO relative to WT. The complete set of microarray data as well a list of the significantly changed genes and more detailed methods have been deposited in the National Center for Biotechnology Gene Expression Omnibus (GEO, http://www.ncbi.nlm.nih.gov/geo/) and are available through GEO accession number GSE19117. The statistical analysis of the data has been reviewed by Dr. Mario Medvedovic, Director of the Division of Biostatistics and Bioinformatics, Department of Environmental Health, University of Cincinnati.

Gene Ontology analysis

Gene Onlology analysis was performed using the online GOrilla program[9] (Gene Ontology enRIchment anaLysis and visuaLizAtion tool) (http://cbl-gorilla.cs.technion.ac.il/). Two analysis options were used: (1) Single Rank List, with the entire gene set ranked according to *P* values; and (2) Two Unranked Lists, in which a target list of genes with a specific range of *P* values is compared against the list of all genes analyzed (13551 total). The Single Rank option avoids setting an arbitrary cutoff of *P* values and was useful for identifying GO categories that were highly enriched at the top end of the significance range. In the Two List analysis, significance and enrichment was calculated based on the number of genes in each GO category that appear in the target list and background list. Enrichment (N, B, n, b) is defined as: N is the total number of genes, B is the total number of genes associated with a specific GO term, n is the number of genes in the top of the user's input list or in the target set when appropriate, b is the number of genes in the intersection; Enrichment = (b/n)/(B/N). The program calculates statistical probabilities using the hypergeometric distribution[9].

Expression atlas data

RNA Seq mRNA expression data for human duodenum and pancreas was obtained from the European Bioinformatics Institute (EBI) Expression Atlas (http://www.ebi.ac.uk/gxa/home). This data base allowed an evaluation of the relative expression levels of the various pancreatic genes that were upregulated in the duodenum of *Nkcc1*$^{-/-}$ mice. The data were available through baseline experiments, Uhlen's lab, in which 32 human tissues are represented.

RESULTS

Upregulation of pancreatic genes in NKCC1-null small intestine

Microarray analysis was performed using small intestine RNA from the *Nkcc1*$^{-/-}$ and WT mice. Among the top 30 genes exhibiting differential expression in the *Nkcc1*-null intestine, all were upregulated, with induction ranging from 3.5-fold to 15.8-fold (Table 2). A pattern of genes typically associated with the exocrine pancreas, namely the digestive enzymes and components of the zymogen granules, was immediately apparent. Cpa1 is a pancreatic carboxypeptidase that was upregulated 15.8-fold. Elastases 1, 2, and 3B were all up-regulated and exhibited high fluorescence intensities. Several serine proteases, including trypsins 1, 2, 4, and 10, as well as chymotrypsins A, B and C, were also up-regulated. Amylase, another digestive enzyme produced by the pancreas, was increased 8.7-fold. Besides digestive enzymes, a number of the highly upregulated genes encode proteins that are associated with zymogen granules (see Discussion). These included glycoprotein 2 (Gp2, 3.9-fold), pancreatic protein disulfide isomerase (Pdia2, 4.5-fold), and syncollin (Sycn, 3.0-fold; $P < 0.001$, data not shown).

In addition to enzymes typical of the exocrine pancreas, genes commonly expressed in the endocrine pancreas were also upregulated. These included Reg1 and Reg2 (regenerating islet or pancreatic stone proteins)[10], which were upregulated 4.6- and 3.6-fold (Table 2), insulin 1 (Ins1, 1.92-fold; $P < 0.003$), and pancreatic-duodenal homeobox 1 (Pdx1; 2.53-fold, $P < 0.002$), which is heavily involved in regulation of β-cell function[11]. Glut2, which is the most abundant facilitative glucose transporter in the intestine[12], was also upregulated (1.65-fold, $P < 0.007$).

Northern blot analysis and quantitative RT-PCR of several genes validated the results of the microarray analysis (Figure 1). The expression of elastase (4.7-fold), amylase (1.9-fold), glycoprotein 2 (3.4-fold), and trypsin (6.0-fold) were all significantly up-regulated in the duodenum (Figure 1A and B). The Northern blot data indicated that the up-regulation of these genes observed in microarray analyses of the *Nkcc1*$^{-/-}$ small intestine occurs primarily in the duodenum. It should be noted that expression of these genes in the duodenum appeared to be robust and did not require long exposure times to be detected, even in the WT samples. RT-PCR confirmed upregulation of Pdx1, Ins1, and Glut2 in the *Nkcc1*$^{-/-}$ small intestine (Figure 1C).

Morphology of the NKCC1-deficient gastrointestinal tract

In previous studies the stomach, intestine, liver, and pancreas of *Nkcc1*$^{-/-}$ mice appeared histologically normal[3], and no apparent differences in the morphology of the gastrointestinal tract was observed in the current study. Based on the results of the microarray analysis and histology, it is evident that the basic population of cells in the intestine of the *Nkcc1*$^{-/-}$ mice is not significantly altered. Expression of the Paneth cell markers matrix metalloproteinase 7 and lysozyme were not significantly changed, and neither were the expression of the major goblet cell markers mucin 2 and TFF3. The expression

Table 2 Genes with the highest levels of differential expression in the *Nkcc1*-null intestine

Gene symbol	Description	Average intensity	Fold change	*P* value
Cpa1	Carboxypeptidase A1, pancreatic	1811	15.86	0.00001
Elane	Elastase 2	2118	12.05	0.00001
Glb1l3	Galactosidase, beta 1 like 3	234	10.27	0.0001
Try4	Trypsin 4	2251	9.91	0.00001
Rnase1	Ribonuclease 1, pancreatic RNase A	592	9.28	0.00001
Cpb1	Carboxypeptidase B1	866	9.15	0.00001
Amy2a5	Amylase 2, pancreatic	691	8.75	0.00001
Try10	Trypsin 10	2306	8.33	0.00001
Ctrc	Chymotrypsin C (caldecrin)	397	7.79	0.0003
Ctrb1	Chymotrypsinogen B1	3360	7.66	0.00001
Pnlip	Pancreatic lipase	1938	7.24	0.00001
Prss1	Protease, serine 1 (trypsin 1)	1481	6.93	0.00001
Cel	Bile salt activated lipase, pancreatic	356	6.73	0.00001
Cela3b	Elastase 3B, pancreatic	1576	6.69	0.00001
Prss2	Protease, serine 2 (trypsin II)	716	6.52	0.0001
Pnliprp1	Pancreatic lipase related protein 1	574	5.83	0.0001
Muc6	Mucin 6, gastric	152	5.78	0.0053
Tff2	Trefoil factor 2	1391	5.77	0.0200
Cela1	Elastase 1, pancreatic	549	4.84	0.0002
V1rh10	Vomeronasal 1 receptor, H10	107	4.66	0.0008
Calb3	Calbindin D9K	609	4.64	0.00001
Reg1	Lithostathine 1 (pancreatic stone protein 1)	5648	4.56	0.0008
Pdia2	Protein disulfide isomerase, pancreatic	292	4.47	0.0004
Akp3	Alkaline phosphatase 3, intestine	366	4.02	0.00001
Gp2	Glycoprotein 2 (zymogen granule membrane)	377	3.92	0.0001
Cep350	Centrosomal protein 350	141	3.92	0.0003
Bmper	BMP-binding endothelial regulator	318	3.78	0.0011
Olfr846	Olfactory receptor 846	432	3.66	0.0001
Reg2	Lithostathine 2 (pancreatic stone protein 2)	253	3.58	0.0383
Ctrl	Chymotrypsin like; chymotrypsin A	1431	3.49	0.0030

Differential expression is presented as fold-changes in *Nkcc1*$^{-/-}$ intestine relative to wild-type intestine. Average intensity (average of Cy3 and Cy5 fluorescence intensities) is roughly indicative of relative expression levels. *P* values are less than or equal to the numbers shown.

of sucrase-isomaltase (alpha glucosidase), associated with terminally-differentiated enterocytes, was also not significantly different. Collectively, these data support the histological assessment that the basic structure and cell populations in the gut of the mutant mice are not significantly changed.

Immunolocalization of pancreatic enzymes in the duodenum

Immunofluorescence of amylase, trypsin, and elastase identified cytoplasmic staining of a subset of cells in the crypts and along the villi. Morphologically, these cells were clearly goblet cells. Co-immunofluorescence experiments using an antibody against intestinal TFF3, which is a goblet-cell specific marker, demonstrated that amylase, elastase and trypsin co-localize with Tff3 in goblet cells (Figure 2). Although mucus is known to bind antibodies non-specifically, in sections containing only the primary or secondary antibody, the goblet cells excluded all background fluorescence, indicating that the staining for each antibody was specific.

Interestingly, all amylase-positive cells contained TFF3; however, not all TFF3-positive cells were amylase-positive. This indicates that only a subset of goblet cells produce pancreatic-type peptidases and auxiliary zymogen granule proteins. Immunolocalization of amylase in cells that were also stained with AB/PAS provided further evidence that expression was occurring in a subset of goblet cells, as there were AB/PAS-positive goblet cells that lacked amylase (Figure 3). In some cases, it was possible to identify an amylase or elastase-positive cloud or cap over the lumenal border of the cells, and above the mucus, suggesting that these proteins are secreted from a separate compartment, or from separate granules, than TFF3-labeled mucins.

Gene Ontology analysis of differentially expressed genes in Nkcc1$^{-/-}$ *intestine*

The differentially expressed genes were subjected to Gene Ontology analysis using the online GOrilla program[9], and significant GO categories were identified (Table 3). Using the single rank option (see Methods), the GO categories included those dealing with digestion and closely related protease and triglyceride lipase activities, which were highly enriched in the top end of the significance range. Sensory perception and the closely related olfactory receptor/G-protein coupled receptor activities were also enriched using the single rank option; these categories included genes spanning a much greater significance range; this was particularly apparent for olfactory receptor activities. Similar results were obtained using the two list option and a

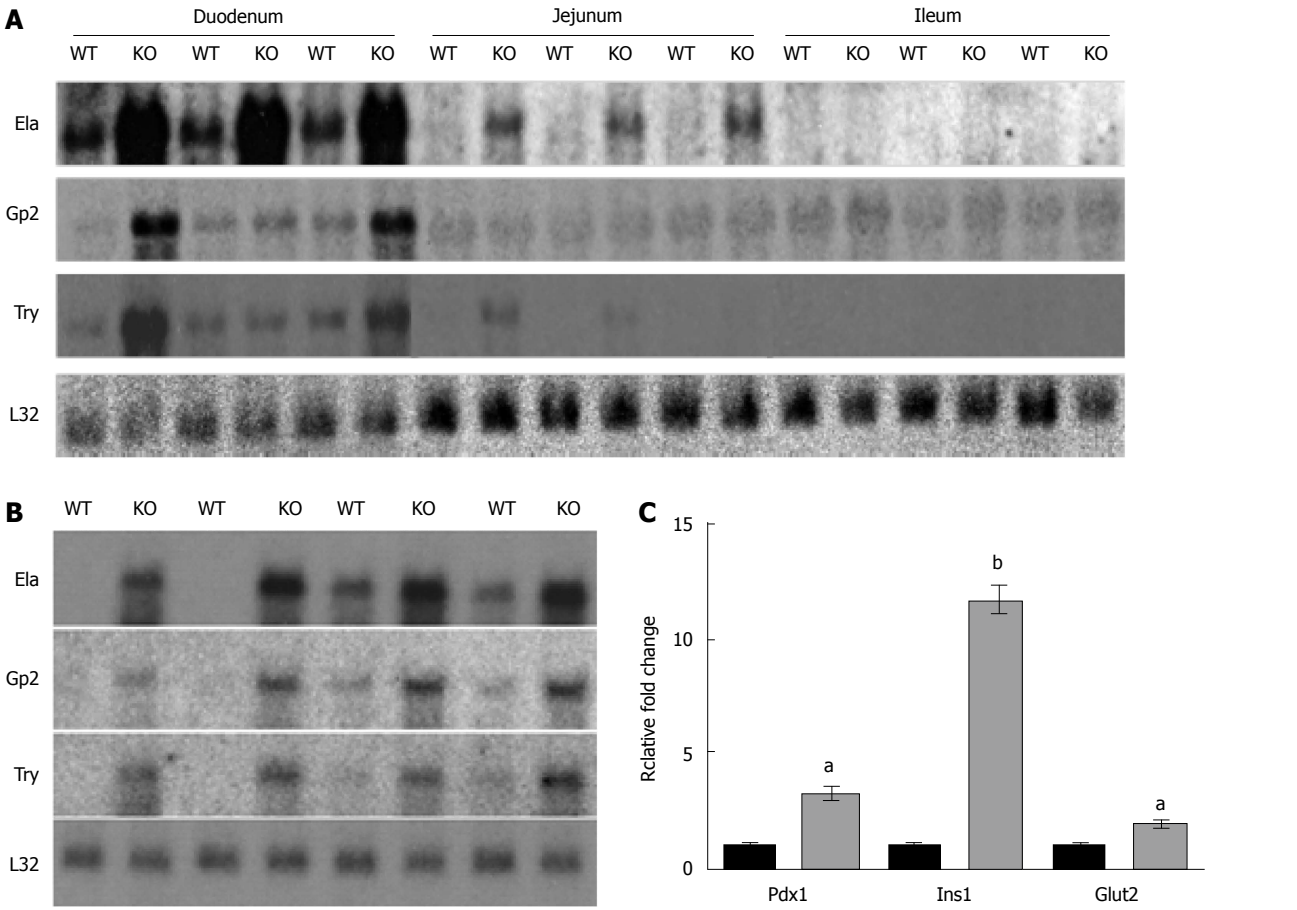

Figure 1 Northern blot and polymerase chain reaction analysis of duodenal gene expression. A: Northern blots show upregulation of Ela, Gp2, and Try primarily in the duodenum of *Nkcc1*$^{-/-}$ (KO) mice relative to WT; *n* = 3 WT and 3 KO for each segment; B: Duodenal tissue from a separate cohort of mice confirms upregulation of elastase (4.7-fold, *P* = 0.002), glycoprotein 2 (3.5-fold, *P* = 0.02) and trypsin (6.0-fold, *P* = 0.002); *n* = 4 WT and 4 KO; C: Quantitative real-time polymerase chain reaction analysis of dx1, Ins1, and Glut2 shows increased expression of these genes in *Nkcc1*$^{-/-}$ duodenum. Expression levels were normalized using the L32 ribosomal subunit mRNA; *n* = 4 WT (black bars) and 4 KO (grey bars). $^{a}P < 0.01$ *vs* WT, $^{b}P < 0.002$ *vs* WT. Gp2: Glycoprotein 2; Ela: Elastase; Try: Trypsin; WT: Wild-type; KO: *Nkcc1*$^{-/-}$; Pdx1: Pancreatic duodenal homeobox 1; Ins1: Insulin1; Glut2: Glucose transporter type 2.

significance cutoff of $P < 0.025$, which analyzed the top 390 genes out of 13551 associated with known GO categories.

The most statistically significant GO categories included genes encoding the pancreatic enzymes that were discussed above, along with genes for additional peptidases and lipases, most of which are directed at digestion of food in the intestinal tract (Table 4). Most of these genes were upregulated; the few that were modestly down-regulated were peptidases with either no apparent role in digestion (*Otud4*, *Dpep3*, and *Hpn*) or that were expressed at very low levels for a digestive enzyme, such as pepsinogen 5.

The most intriguing changes involved altered expression of receptors involved in chemical sensing (Table 5). These included some G-protein coupled receptors (GPCRs) that are known to be involved in chemical sensing in the intestinal tract, such as Gpbar1[13] and Ffar2[14], as well as a large number of G-protein receptors of the olfactory receptor family and several of the vomeronasal receptor family. As discussed below, this suggests that the loss of NKCC1 affects chemosensing in the intestinal tract, and also suggests that olfactory and vomeronasal receptors play a major role in this process.

DISCUSSION

The results of this study show that the loss of NKCC1 in small intestine leads to upregulation of digestive enzymes, many of which are typical of the exocrine pancreas, and to differential expression of a large number of genes encoding chemosensing receptors. As noted in the Introduction, loss-of-function mutations in the *SLC12A2* (NKCC1) gene lead to unexplained failure of intestinal function/food tolerance (http://www.genome.gov/27551936). Although it is possible that impaired secretion contributes to this phenotype, considerable compensation for loss of NKCC1-mediated basolateral Cl^--uptake occurs in the intestine[5,6] and Cystic Fibrosis patients and mice exhibit a more profound secretory defect than NKCC1-null mice. This suggests that factors other than impaired secretion account for the severe intestinal phenotype in humans with *Nkcc1* mutations.

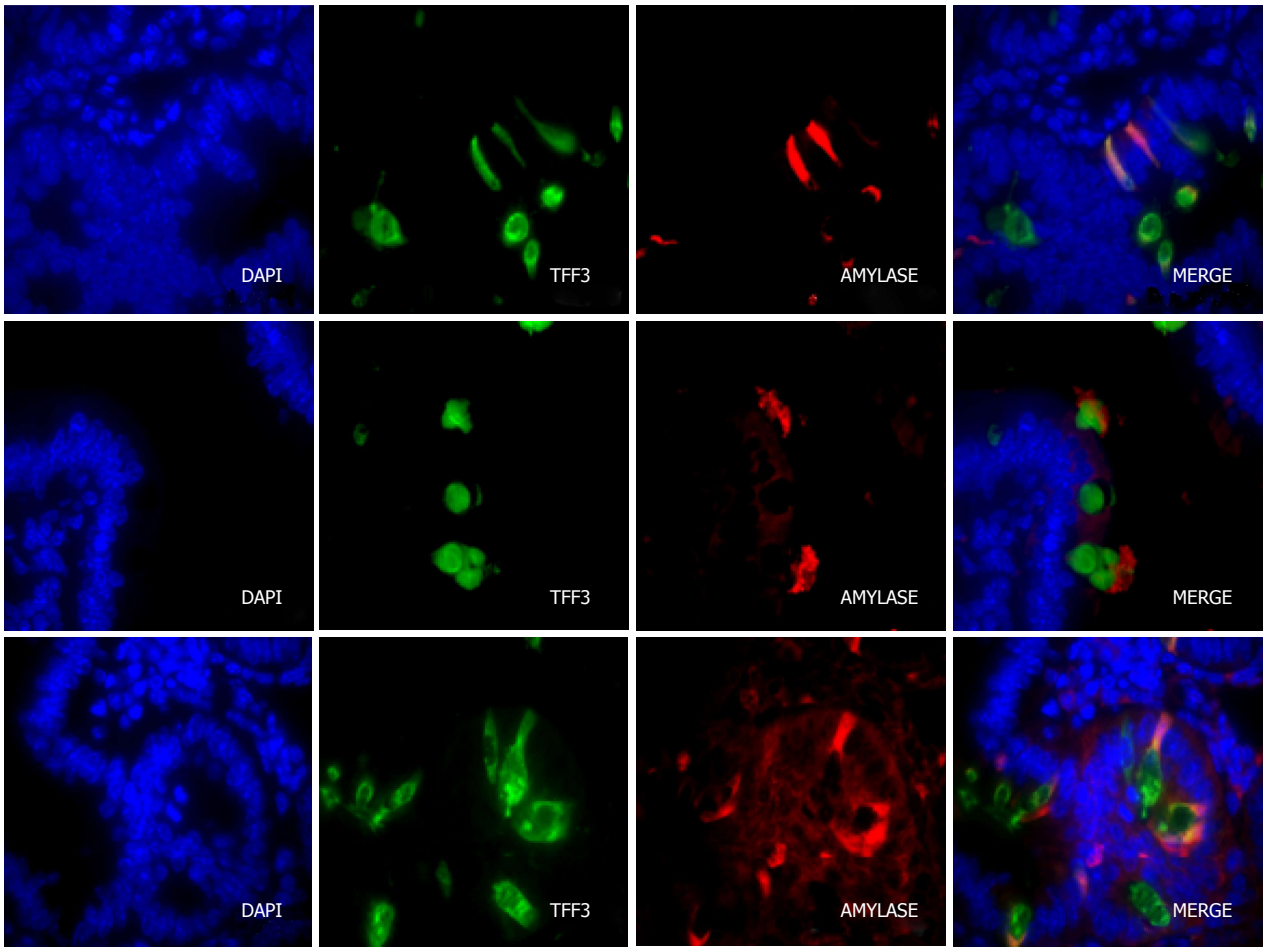

Figure 2 Colocalization of peptidases in goblet cells of the duodenum. DAPI (blue) identifies nuclei and TFF3 (intestinal trefoil factor, green fluorescence) identifies goblet cells. Elastase, amylase and trypsin are identified by red fluorescence. The merged images show colocalization of each of these proteases and TFF3. Staining patterns were assessed in 4 wild-type and 3 *Nkcc1*$^{-/-}$ mice. The images shown are for NKCC1-null mice. Control sections with only primary or only secondary antibodies do not identify goblet cells (not shown).

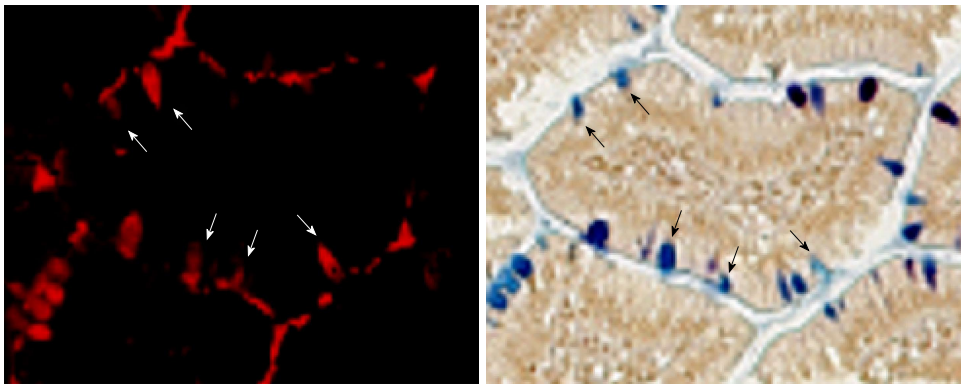

Figure 3 Amylase is expressed in a subset of goblet cells. Immunofluorescence of amylase (top, red) identifies many, but not all, goblet cells that are clearly stained with AB/PAS (bottom). The same sections (slides) from NKCC1-null intestine was used for immunofluorescence, imaged, and then stained with AB/PAS. Arrows indicate the same cell in both images. AB/PAS: Alcian Blue/Periodic Acid-Schiff.

The most striking result of the microarray analyses, although perhaps of limited clinical importance (discussed below), was the increased expression of digestive enzymes that are normally expressed at high levels in the pancreas and the restriction of their expression to a subset of goblet cells. Because it is critical to prevent premature release of digestive enzymes within the pancreas, many digestive enzymes are produced and packaged as inactive forms in zymogen granules, which release the enzymes upon secretion into the duodenum. Several genes that encode proteins involved in zymogen granule function (Gp2, Sync, and Pdia2),

Table 3 Significantly enriched Gene Ontology categories

GO category	*P*-value	Enrichment	(*N*, B, *n*, b)
Single ranked list			
GO:0008236 Serine-type peptidase activity	3.38E-14	35.6	(13551, 135, 31, 11)
GO:0008233 Peptidase activity	7.66E-11	12.6	(13551, 451, 31, 13)
GO:0007586 Digestion	1.82E-10	209.8	(13551, 19, 17, 5)
GO:0007600 Sensory perception	3.45E-8	1.67	(13551, 817, 1270, 128)
GO:0006508 Proteolysis	4.01E-8	7.65	(13551, 743, 31, 13)
GO:0004984 Olfactory receptor activity	7.11E-8	1.82	(13551, 552, 1270, 94)
GO:0004806 Triglyceride lipase activity	7.01E-7	271.0	(13551, 10, 15, 3)
GO:0004930 GPCR activity	3.86E-5	2.41	(13551, 512, 352, 32)
Two unranked lists (target and background)			
GO:0008236 Serine-type peptidase activity	6.03E-8	4.63	(13551, 135, 390, 18)
GO:0007586 Digestion	5.79E-7	12.8	(13551, 19, 390, 7)
GO:0004930 GPCR activity	1.30E-5	2.24	(13551, 512, 390, 33)
GO:0004984 Olfactory receptor activity	5.86E-5	2.08	(13551, 552, 390,3 3)
GO:0004806 Triglyceride lipase activity	1.24E-4	13.9	(13551, 10, 390, 4)
GO:0008233 Peptidase activity	2.71E-4	2.08	(13551, 451, 390, 27)

GO categories were identified using both the Single rank and Two unranked list options of the GOrilla Gene Ontology program[9]. *N* is the total number of genes, B is the total number of genes associated with a specific GO term, *n* is the number of genes in the target set, b is the number of genes in the intersection. Enrichment = (b/*n*)/(B/*N*). GPCR: G-protein coupled receptor; GO: Gene Ontology.

Table 4 Digestive enzymes and peptidases altered in small intestine of *Nkcc1*$^{-/-}$ mice

Gene symbol	Description	Average intensity	Fold change	*P*-value
Cpa1	Carboxypeptidase A1, pancreatic	1811	15.86	0.00001
Elane	Elastase 2	2118	12.05	0.00001
Try4	Trypsin 4	2251	9.91	0.00001
Cpb1	Carboxypeptidase B1 (tissue)	866	9.15	0.00001
Try10	Trypsin 10	2306	8.33	0.00001
Ctrc	Chymotrypsin C (caldecrin)	397	7.79	0.0003
Ctrb1	Chymotrypsinogen B	3360	7.66	0.00001
Pnlip	Pancreatic lipase	1938	7.24	0.00001
Prss1	Protease, serine 1 (trypsin 1)	1481	6.93	0.00001
Cel	Carboxyester lipase, pancreatic	356	6.73	0.00001
Cela3b	Elastase 3B, pancreatic	1576	6.69	0.00001
Prss2	Trypsin Ⅱ, anionic	716	6.52	0.0001
Pnliprp1	Pancreatic lipase related protein 1	574	5.83	0.0001
Cela1	Elastase 1, pancreatic	549	4.84	0.0002
2210010C04Rik	RIKEN cDNA 2210010C04 gene	125	3.89	0.0005
Ctrl	Chymotrypsin like; chymotrypsin A	1431	3.49	0.0030
Klk1	Kallikrein 1	278	1.82	0.0180
Klk1b26	Kallikrein 1-related petidase b26	988	1.80	0.0030
Pnliprp2	Pancreatic lipase related protein 2	833	1.74	0.0181
Klk1b21	Kallikrein 21	386	1.66	0.0036
Cyp7b1	Cytochrome P450 7B1	100	1.53	0.0229
Prcp	Prolyl carboxypeptidase (angiotensinase C)	566	1.51	0.0047
Amz1	Archaelysin family metallopeptidase 1	887	1.35	0.0121
Otud4	OTU domain containing 4	524	-1.34	0.0221
Pga5	Pepsinogen 5, group Ⅰ	168	-1.42	0.0198
Dpep3	Dipeptidase 3	301	-1.48	0.0197
Hpn	Serine protease hepsin	206	-1.99	0.0211

Differential expression is presented as fold-changes in *Nkcc1*$^{-/-}$ intestine relative to wild-type intestine. Average intensity (average of Cy3 and Cy5 fluorescence intensities) is roughly indicative of relative expression levels. *P* values are less than or equal to the numbers shown.

were upregulated. Glycoprotein 2 is the most abundant protein on zymogen granules and is thought to regulate exocytosis at the apical pole of the granule[15]. Syncollin is found on the luminal surface of zymogen granules, and syncollin-deficient mice exhibit impaired exocytosis of granules from pancreatic acinar cells[16]. Pancreatic protein disulfide isomerase plays a major role in forming the disulfide linkages of secretory proteins and has been localized to zymogen granule membranes[17]. These expression patterns are consistent with increased synthesis and packaging of zymogen granule proteins in the *Nkcc1*$^{-/-}$ intestine.

During embryonic development, the endoderm gives rise to the pancreas, liver, and the epithelial

Table 5 G-protein coupled, olfactory, and vomeronasal receptors

Gene symbol	Description	Average intensity	Fold change	*P*-value
V1rh10	Vomeronasal 1 receptor, H10	107	4.66	0.0008
Olfr846	Olfactory receptor 846	432	3.66	0.0001
Olfr491	Olfactory receptor 491	79	3.18	0.0051
Olfr419	Olfactory receptor 419	477	3.12	0.0004
Olfr827	Olfactory receptor 827	122	2.65	0.0001
Olfr992	Olfactory receptor 992	300	2.53	0.0005
Olfr506	Olfactory receptor 506	143	2.48	0.0049
Olfr812	Olfactory receptor 812	53	2.37	0.0048
Gpr63	G protein-coupled receptor 63	42	2.08	0.0023
Olfr1080	Olfactory receptor 1080	66	1.90	0.0107
V1rh1	Vomeronasal 1 receptor, H2	60	1.88	0.0071
Olfr344	Olfactory receptor 344	50	1.87	0.0057
Olfr1340	Olfactory receptor 1340	79	1.83	0.0123
Olfr378	Olfactory receptor 378	67	1.81	0.0072
Olfr643	Olfactory receptor 643	77	1.72	0.0080
Olfr1000	Olfactory receptor 996	475	1.72	0.0127
Olfr1134	Olfactory receptor 1134	139	1.71	0.0101
Olfr906	Olfactory receptor 906	134	1.68	0.0038
Olfr736	Olfactory receptor 736	92	1.67	0.0166
Olfr433	Olfactory receptor 433	189	1.65	0.0039
Olfr78	Olfactory receptor 78	125	1.62	0.0087
Olfr90	Olfactory receptor 90	106	1.56	0.0235
Prokr1	Prokineticin receptor 1	196	1.56	0.0096
Olfr1494	Olfactory receptor 1494	457	1.54	0.0180
Olfr1462	Olfactory receptor 1462	260	1.52	0.0183
Olfr444	Olfactory receptor 444	252	1.52	0.0154
Nmur1	Neuromedin U receptor 1	196	1.51	0.0177
Olfr1366	Olfactory receptor 1366	89	1.50	0.0207
Olfr804	Olfactory receptor 804	404	1.48	0.0175
Gpbar1	G protein-coupled bile acid receptor 1	129	1.47	0.0216
Gprc5a	G protein-coupled receptor, C5A	936	1.46	0.0142
Olfr740	Olfactory receptor 739	172	1.43	0.0164
Olfr1156	Olfactory receptor 152	156	1.43	0.0211
Rxfp4	Relaxin family peptide receptor 4	397	1.37	0.0132
Igf2r	Insulin-like growth factor 2 receptor	1089	-1.39	0.0158
Olfr641	Olfactory receptor 641	652	-1.39	0.0211
Olfr48	Olfactory receptor 140	99	-1.48	0.0143
Vmn1r210	Vomeronasal 1 receptor 210	192	-1.54	0.0127
Grm2	Glutamate receptor, metabotropic 2	179	-1.63	0.0028
Vmn1r5	Vomeronasal 1 receptor 5	124	-1.64	0.0071
Ffar2	Free fatty acid receptor 2	203	-1.85	0.0092

Differential expression is presented as fold-changes in *Nkcc1*$^{-/-}$ intestine relative to wild-type intestine. Average intensity (average of Cy3 and Cy5 fluorescence intensities) is roughly indicative of relative expression levels. *P* values are less than or equal to the numbers shown.

lining of the gastrointestinal tract. This requires the expression of various transcription factors, as well as interactions between the epithelium and surrounding mesenchyme[18,19]. It has become clear that the relative plasticity of the pancreas, liver, and intestine is high, and that certain populations of cells within these organs can undergo transdifferentiation. Although this initially seemed to be an interesting possibility, it is unlikely that transdifferentiation is occurring in the *Nkcc1*$^{-/-}$ small intestine. Several transcription factors, including Pdx1 and pancreas transcription factor 1 (Ptf1a) have been shown to mediate plasticity between the pancreas and small intestine. Expression of Pdx1 is a key regulatory step in the development of both the pancreas and the duodenum[20], and inactivation of Ptf1a drives pancreatic precursor cells toward intestinal cell fates[21]. Although expression of pancreatic genes was upregulated, Pdx1 was only modestly increased and expression of Ptf1a was not changed (data not shown). Furthermore, when we examined relative expression levels of the pancreatic enzymes in human pancreas and duodenum that are available through the EBI Expression Atlas (see methods) it was clear that the pancreatic enzymes are expressed at several orders of magnitude higher levels in pancreas than in duodenum. Thus, the apparently robust expression of pancreatic enzymes in the *Nkcc1*$^{-/-}$ intestine is likely to be far below the levels of expression occurring in the pancreas. Similarly, although insulin (Ins1) was mildly induced in *Nkcc1*$^{-/-}$ intestine, the EBI expression Atlas data indicates that insulin expression in human pancreas is far greater than that in duodenum (relative transcript levels 551 in pancreas *vs* 0.3 in duodenum). Although we obtained an antibody against human insulin, which readily and specifically identified

pancreatic islet cells in the mouse (data not shown), we were unable to detect insulin in *Nkcc1*$^{-/-}$ intestine, consistent with exceedingly low levels of expression.

The reason for the increased expression of pancreatic enzymes in goblet cells is unclear. Histological analyses gave no evidence for an increase in goblet cells in *Nkcc1*$^{-/-}$ intestine, and the expression levels of Tff3 (intestinal trefoil factor) and Muc2 (mucin 2), which are expressed at very high levels in goblet cells, were not significantly changed. However, NKCC1 has been shown to be expressed at high levels on basolateral membranes of goblet cells[1], and there is evidence that it affects mucous secretion[22]. Thus, it is possible that the absence of NKCC1 specifically in goblet cells has a direct effect on the expression of pancreatic enzymes. Whether this is due to subtle effects of NKCC1-deficiency on the differentiation of goblet cells is unclear.

Despite the changes in mRNA expression patterns between the WT and *Nkcc1*$^{-/-}$ intestine, previous studies of two different NKCC1 knockouts revealed no significant histological changes between the two genotypes in the adult intestine[3,4]. Furthermore, detailed morphometric analyses of the intestinal tracts of 8-wk-old WT and *Nkcc1*$^{-/-}$ mice, the same age as used in the current study, revealed no significant differences in cell structure[3]. We cannot, of course, rule out subtle changes in cell differentiation resulting from changes during early development or during regular turnover of the epithelium. However, the normal epithelial cell structure and relatively modest changes in expression of two of the major transcription factors involved in development of the pancreas and intestine, argue against defects in development and/or epithelial cell differentiation as the basis of the observed expression changes. Also, as discussed below, NKCC1 serves a direct role in the process of chemical sensing in olfactory neurons, suggesting that the changes in expression of chemosensing receptors is a direct response to the absence NKCC1 rather than being secondary to developmental defects.

Although less dramatic than the changes in pancreatic genes, the significant changes in expression of a large number of G-protein coupled chemosensing receptors suggest that the loss of NKCC1 may cause major impairments in the sensing of nutrients and other constituents of the intestinal contents. It is clear from many studies that GPCRs play a major role in intestinal chemosensing[23]. In fact, some of the GPCRs identified as differentially expressed in our microarray analyses have been shown to play important roles in chemosensing in the gut. Gpbar1 (1.47-fold increase) is expressed in enteroendocrine L-cells, where it senses bile acids and transduces a signal that leads to secretion of glucagon-like peptide 1 (GLP-1) and peptide tyrosine-tyrosine, thereby regulating glucose homeostasis[13,24]. Ffar2 (-1.85-fold decrease) is expressed in enteroendocrine cells and serves as a sensor of short-chain fatty acids[14]. Gpr63 (2.1-fold increase), which was expressed at relatively low levels, has been identified as a receptor for several lipids, including N-Arachidonylethanolamine[25] and both sphingosine 1-phosphate and dioleoylphasphatidic acid[26]. Grm2 (-1.63-fold decrease) is one of the metabotropic glutamate receptors that is involved in nutrient sensing through taste receptors[27]. Several of the differentially expressed GPCRs serve as receptors for peptide hormones that affect gut function. These include Rxfp4 (1.37-fold increase), which is the receptor for the orexigenic (appetite-stimulating) insulin-like peptide 5[28], and Nmur1 (1.51-fold increase), which is a receptor for neuromedin U and functions in glucose and appetite homeostasis[29].

The GPCRs that are known to play major roles in chemical sensing include taste receptors, olfactory receptors, and volmeronasal receptors. Taste receptors are known to function in the intestinal tract and to play major roles in nutrient sensing and subsequent signaling events[27,30-32]. There is less information about the role of olfactory receptors in chemosensing in the intestinal tract, but recent evidence indicates that olfactory receptors are expressed on colonic epithelial tissues, where they may detect bacterial metabolites in the luminal contents[33]. In addition, specific olfactory receptors have been shown to be differentially expressed in the duodenum of obesity-prone rats fed a high-fat diet[34]. The authors speculated that these receptors may be involved in sensing and responding to dietary fat. Specific olfactory receptors have also been identified in human enterochromaffin cells and when stimulated can lead to the release of serotonin[35,36]. Vomeronasal receptors also function in chemosensing[37], but as far as we are aware there is no previous evidence for their expression and function in the intestinal tract. Nevertheless, V1rh10 was the most highly upregulated gene among the G-protein coupled receptors (4.66-fold), indicating that it's expression is responsive to the loss of NKCC1.

Previous studies have shown that NKCC1 plays an important role in signaling through olfactory receptors. Odorant-induced Cl^- currents, which are required for signaling, were reduced in olfactory neurons of *Nkcc1*$^{-/-}$ mice[38], indicating that NKCC1 is an important mechanism for Cl^--uptake in olfactory neurons. However, later studies provided strong evidence for additional Cl^--loading mechanisms that can provide some compensation for the loss of NKCC1[39,40], and physiological studies indicated that WT and *Nkcc1*$^{-/-}$ mice have similar sensitivities to several specific odorants[41]. In more recent studies, however, loss of NKCC1 caused defects in the sensitivity to a complex mixture of odorants, and RNA Seq analysis of WT and *Nkcc1*$^{-/-}$ olfactory epithelium revealed significant differential expression changes involving a large number of olfactory receptors[42]. Thus, loss of NKCC1 leads to differential expression changes involving chemosensing receptors in both the olfactory epithelium[42] and in the small intestine, as indicated in the current study.

In summary, the microarray analysis of *Nkcc1*$^{-/-}$ small intestine indicates that the loss of NKCC1 leads both to increased expression of pancreatic enzymes in a subset of goblet cells and to differential expression of chemosensing GPCRs, including a large number of olfactory receptors. Because a number of GPCRs with well-established roles in chemosensing in the intestine were among the receptors that were changed, it seems likely that the differential expression of olfactory receptors is also indicative of altered sensing of components of the luminal contents. This finding raises the possibility that the episodic hypoglycemia and failure of intestinal function/food tolerance observed in human patients with NKCC1 (*SLC12A2* gene) mutations may be due to chronic deficiencies in their ability to properly sense and respond to nutrients and other constituents of the intestinal lumen. Finally, it should also be noted that loop diuretics that inhibit NKCC1 have been associated with an increased incidence of intestinal dysfunction, including constipation[43] and indications of a poor outcome following ischemic colitis[44]. It is therefore possible that inhibition of NKCC1 by these common therapeutic agents could lead to intestinal dysfunction similar to that observed in NKCC1 genetic deficiencies. Whether this is due to developmental abnormalities involving one or more cell types in the intestinal epithelium and/or is a more direct response to impaired chemosensing is unclear.

COMMENTS

Background

In the intestine, the basolateral NKCC1 Na^+-K^+-$2Cl^-$ cotransporter is the major mechanism of chloride uptake in support of secretion; however, it is not restricted to secretory epithelia and may serve other functions as well. To gain insights regarding novel functions of NKCC1 in the intestine, mRNA expression patterns in wild-type and NKCC1-null intestine were analyzed.

Research frontiers

This study was designed to determine changes in gene expression occurring in the intestinal tract of mice lacking NKCC1. Analysis of those patterns provided evidence that NKCC1 plays an important role in chemical sensing in the intestinal tract, a relatively new area of investigation.

Innovations and breakthroughs

This study demonstrates for the first time that mRNA levels for a large number of olfactory receptors and other G-protein coupled receptors involved in chemical sensing in the intestinal tract are altered in response to the loss of NKCC1.

Applications

The effects of *NKCC1* ablation on the expression of large numbers of chemosensory receptors raises the possibility that the failure of intestinal function in response to genetic mutations in the human *NKCC1* gene and side effects of loop diuretic treatment in the intestine could be due in part to impaired chemical sensing.

Terminology

The *Slc12a2* gene, encoding the NKCC1 Na^+-K^+-$2Cl^-$ cotransporter, was genetically ablated in the mouse model used in this study. The corresponding human gene is *SLC12A2*; mutations in human *SLC12A2* gene have been shown to cause failure of intestinal function.

Peer-review

This study aimed to analyze the mRNA expression changes in the intestine of *NKCC1*$^{-/-}$ mice. The methods of this study, methods were properly used to identify cell types, and results were also presented clearly.

REFERENCES

1 **Jakab RL**, Collaco AM, Ameen NA. Physiological relevance of cell-specific distribution patterns of CFTR, NKCC1, NBCe1, and NHE3 along the crypt-villus axis in the intestine. *Am J Physiol Gastrointest Liver Physiol* 2011; **300**: G82-G98 [PMID: 21030607 DOI: 10.1152/ajpgi.00245.2010]

2 **Clarke LL**, Gawenis LR, Franklin CL, Harline MC. Increased survival of CFTR knockout mice with an oral osmotic laxative. *Lab Anim Sci* 1996; **46**: 612-618 [PMID: 9001172]

3 **Flagella M**, Clarke LL, Miller ML, Erway LC, Giannella RA, Andringa A, Gawenis LR, Kramer J, Duffy JJ, Doetschman T, Lorenz JN, Yamoah EN, Cardell EL, Shull GE. Mice lacking the basolateral Na-K-2Cl cotransporter have impaired epithelial chloride secretion and are profoundly deaf. *J Biol Chem* 1999; **274**: 26946-26955 [PMID: 10480906 DOI: 10.1074/jbc.274.38.26946]

4 **Grubb BR**, Lee E, Pace AJ, Koller BH, Boucher RC. Intestinal ion transport in NKCC1-deficient mice. *Am J Physiol Gastrointest Liver Physiol* 2000; **279**: G707-G718 [PMID: 11005757]

5 **Walker NM**, Flagella M, Gawenis LR, Shull GE, Clarke LL. An alternate pathway of cAMP-stimulated Cl secretion across the NKCC1-null murine duodenum. *Gastroenterology* 2002; **123**: 531-541 [PMID: 12145806]

6 **Gawenis LR**, Bradford EM, Alper SL, Prasad V, Shull GE. AE2 Cl-/HCO3- exchanger is required for normal cAMP-stimulated anion secretion in murine proximal colon. *Am J Physiol Gastrointest Liver Physiol* 2010; **298**: G493-G503 [PMID: 20110461 DOI: 10.1152/ajpgi.00178]

7 **Woo AL**, Gildea LA, Tack LM, Miller ML, Spicer Z, Millhorn DE, Finkelman FD, Hassett DJ, Shull GE. In vivo evidence for interferon-gamma-mediated homeostatic mechanisms in small intestine of the NHE3 Na+/H+ exchanger knockout model of congenital diarrhea. *J Biol Chem* 2002; **277**: 49036-49046 [PMID: 12370192]

8 **Bradford EM**, Sartor MA, Gawenis LR, Clarke LL, Shull GE. Reduced NHE3-mediated Na+ absorption increases survival and decreases the incidence of intestinal obstructions in cystic fibrosis mice. *Am J Physiol Gastrointest Liver Physiol* 2009; **296**: G886-G898 [PMID: 19164484 DOI: 10.1152/ajpgi.90520]

9 **Eden E**, Navon R, Steinfeld I, Lipson D, Yakhini Z. GOrilla: a tool for discovery and visualization of enriched GO terms in ranked gene lists. *BMC Bioinformatics* 2009; **10**: 48 [PMID: 19192299 DOI: 10.1186/1471-2105-10-48]

10 **Qiu L**, List EO, Kopchick JJ. Differentially expressed proteins in the pancreas of diet-induced diabetic mice. *Mol Cell Proteomics* 2005; **4**: 1311-1318 [PMID: 15961380 DOI: 10.1074/mcp.M500016-MCP200]

11 **Kaneto H**, Matsuoka TA, Miyatsuka T, Kawamori D, Katakami N, Yamasaki Y, Matsuhisa M. PDX-1 functions as a master factor in the pancreas. *Front Biosci* 2008; **13**: 6406-6420 [PMID: 18508668]

12 **Thorens B**. GLUT2, glucose sensing and glucose homeostasis. *Diabetologia* 2015; **58**: 221-232 [PMID: 25421524 DOI: 10.1007/s00125-014-3451-1]

13 **Ullmer C**, Alvarez Sanchez R, Sprecher U, Raab S, Mattei P, Dehmlow H, Sewing S, Iglesias A, Beauchamp J, Conde-Knape K. Systemic bile acid sensing by G protein-coupled bile acid receptor 1 (GPBAR1) promotes PYY and GLP-1 release. *Br J Pharmacol* 2013; **169**: 671-684 [PMID: 23488746 DOI: 10.1111/bph.12158]

14 **Nøhr MK**, Pedersen MH, Gille A, Egerod KL, Engelstoft MS, Husted AS, Sichlau RM, Grunddal KV, Poulsen SS, Han S, Jones RM, Offermanns S, Schwartz TW. GPR41/FFAR3 and GPR43/FFAR2 as cosensors for short-chain fatty acids in enteroendocrine cells vs FFAR3 in enteric neurons and FFAR2 in enteric leukocytes. *Endocrinology* 2013; **154**: 3552-3564 [PMID: 23885020 DOI: 10.1210/en.2013-1142]

15 **Parker EM**, Zaman MM, Freedman SD. GP2, a GPI-anchored protein in the apical plasma membrane of the pancreatic acinar cell, co-immunoprecipitates with src kinases and caveolin. *Pancreas* 2000; **21**: 219-225 [PMID: 11039464]

16 **Wäsle B**, Turvey M, Larina O, Thorn P, Skepper J, Morton AJ, Edwardson JM. Syncollin is required for efficient zymogen granule exocytosis. *Biochem J* 2005; **385**: 721-727 [PMID: 15462671]

17 **Bruneau N**, Lombardo D, Levy E, Bendayan M. Roles of molecular chaperones in pancreatic secretion and their involvement in intestinal absorption. *Microsc Res Tech* 2000; **49**: 329-345 [PMID: 10820517]

18 **Montgomery RK**, Mulberg AE, Grand RJ. Development of the human gastrointestinal tract: twenty years of progress. *Gastroenterology* 1999; **116**: 702-731 [PMID: 10029630]

19 **Stainier DY**. No organ left behind: tales of gut development and evolution. *Science* 2005; **307**: 1902-1904 [PMID: 15790841]

20 **Offield MF**, Jetton TL, Labosky PA, Ray M, Stein RW, Magnuson MA, Hogan BL, Wright CV. PDX-1 is required for pancreatic outgrowth and differentiation of the rostral duodenum. *Development* 1996; **122**: 983-995 [PMID: 8631275]

21 **Kawaguchi Y**, Cooper B, Gannon M, Ray M, MacDonald RJ, Wright CV. The role of the transcriptional regulator Ptf1a in converting intestinal to pancreatic progenitors. *Nat Genet* 2002; **32**: 128-134 [PMID: 12185368]

22 **Dolganov GM**, Woodruff PG, Novikov AA, Zhang Y, Ferrando RE, Szubin R, Fahy JV. A novel method of gene transcript profiling in airway biopsy homogenates reveals increased expression of a Na+-K+-Cl- cotransporter (NKCC1) in asthmatic subjects. *Genome Res* 2001; **11**: 1473-1483 [PMID: 11544191]

23 **Reimann F**, Tolhurst G, Gribble FM. G-protein-coupled receptors in intestinal chemosensation. *Cell Metab* 2012; **15**: 421-431 [PMID: 22482725 DOI: 10.1016/j.cmet.2011.12.019]

24 **Thomas C**, Gioiello A, Noriega L, Strehle A, Oury J, Rizzo G, Macchiarulo A, Yamamoto H, Mataki C, Pruzanski M, Pellicciari R, Auwerx J, Schoonjans K. TGR5-mediated bile acid sensing controls glucose homeostasis. *Cell Metab* 2009; **10**: 167-177 [PMID: 19723493 DOI: 10.1016/j.cmet.2009.08.001]

25 **Yin H**, Chu A, Li W, Wang B, Shelton F, Otero F, Nguyen DG, Caldwell JS, Chen YA. Lipid G protein-coupled receptor ligand identification using beta-arrestin PathHunter assay. *J Biol Chem* 2009; **284**: 12328-12338 [PMID: 19286662 DOI: 10.1074/jbc.M806516200]

26 **Niedernberg A**, Tunaru S, Blaukat A, Ardati A, Kostenis E. Sphingosine 1-phosphate and dioleoylphosphatidic acid are low affinity agonists for the orphan receptor GPR63. *Cell Signal* 2003; **15**: 435-446 [PMID: 12618218]

27 **Xiao W**, Feng Y, Holst JJ, Hartmann B, Yang H, Teitelbaum DH. Glutamate prevents intestinal atrophy via luminal nutrient sensing in a mouse model of total parenteral nutrition. *FASEB J* 2014; **28**: 2073-2087 [PMID: 24497581 DOI: 10.1096/fj.13-238311]

28 **Grosse J**, Heffron H, Burling K, Akhter Hossain M, Habib AM, Rogers GJ, Richards P, Larder R, Rimmington D, Adriaenssens AA, Parton L, Powell J, Binda M, Colledge WH, Doran J, Toyoda Y, Wade JD, Aparicio S, Carlton MB, Coll AP, Reimann F, O'Rahilly S, Gribble FM. Insulin-like peptide 5 is an orexigenic gastrointestinal hormone. *Proc Natl Acad Sci USA* 2014; **111**: 11133-11138 [PMID: 25028498 DOI: 10.1073/pnas.1411413111]

29 **Dalbøge LS**, Pedersen SL, Secher T, Holst B, Vrang N, Jelsing J. Neuromedin U inhibits food intake partly by inhibiting gastric emptying. *Peptides* 2015; **69**: 56-65 [PMID: 25895852 DOI: 10.1016/j.peptides.2015.04.010]

30 **Mace OJ**, Lister N, Morgan E, Shepherd E, Affleck J, Helliwell P, Bronk JR, Kellett GL, Meredith D, Boyd R, Pieri M, Bailey PD, Pettcrew R, Foley D. An energy supply network of nutrient absorption coordinated by calcium and T1R taste receptors in rat small intestine. *J Physiol* 2009; **587**: 195-210 [PMID: 19001049 DOI: 10.1113/jphysiol.2008.159616]

31 **Wang JH**, Inoue T, Higashiyama M, Guth PH, Engel E, Kaunitz JD, Akiba Y. Umami receptor activation increases duodenal bicarbonate secretion via glucagon-like peptide-2 release in rats. *J Pharmacol Exp Ther* 2011; **339**: 464-473 [PMID: 21846840 DOI: 10.1124/jpet.111.184788]

32 **Rønnestad I**, Akiba Y, Kaji I, Kaunitz JD. Duodenal luminal nutrient sensing. *Curr Opin Pharmacol* 2014; **19**: 67-75 [PMID: 25113991 DOI: 10.1016/j.coph.2014.07.010]

33 **Kaji I**, Karaki S, Kuwahara A. Taste sensing in the colon. *Curr Pharm Des* 2014; **20**: 2766-2774 [PMID: 23886384]

34 **Primeaux SD**, Braymer HD, Bray GA. High fat diet differentially regulates the expression of olfactory receptors in the duodenum of obesity-prone and obesity-resistant rats. *Dig Dis Sci* 2013; **58**: 72-76 [PMID: 23053893 DOI: 10.1007/s10620-012-2421-z]

35 **Braun T**, Voland P, Kunz L, Prinz C, Gratzl M. Enterochromaffin cells of the human gut: sensors for spices and odorants. *Gastroenterology* 2007; **132**: 1890-1901 [PMID: 17484882]

36 **Kidd M**, Modlin IM, Gustafsson BI, Drozdov I, Hauso O, Pfragner R. Luminal regulation of normal and neoplastic human EC cell serotonin release is mediated by bile salts, amines, tastants, and olfactants. *Am J Physiol Gastrointest Liver Physiol* 2008; **295**: G260-G272 [PMID: 18556422 DOI: 10.1152/ajpgi.00056.2008]

37 **Chamero P**, Leinders-Zufall T, Zufall F. From genes to social communication: molecular sensing by the vomeronasal organ. *Trends Neurosci* 2012; **35**: 597-606 [PMID: 22658923 DOI: 10.1016/j.tins.2012.04.011]

38 **Reisert J**, Lai J, Yau KW, Bradley J. Mechanism of the excitatory Cl- response in mouse olfactory receptor neurons. *Neuron* 2005; **45**: 553-561 [PMID: 15721241]

39 **Nickell WT**, Kleene NK, Gesteland RC, Kleene SJ. Neuronal chloride accumulation in olfactory epithelium of mice lacking NKCC1. *J Neurophysiol* 2006; **95**: 2003-2006 [PMID: 16319203]

40 **Nickell WT**, Kleene NK, Kleene SJ. Mechanisms of neuronal chloride accumulation in intact mouse olfactory epithelium. *J Physiol* 2007; **583**: 1005-1020 [PMID: 17656441]

41 **Smith DW**, Thach S, Marshall EL, Mendoza MG, Kleene SJ. Mice lacking NKCC1 have normal olfactory sensitivity. *Physiol Behav* 2008; **93**: 44-49 [PMID: 17719611]

42 **Haering C**, Kanageswaran N, Bouvain P, Scholz P, Altmüller J, Becker C, Gisselmann G, Wäring-Bischof J, Hatt H. Ion transporter NKCC1, modulator of neurogenesis in murine olfactory neurons. *J Biol Chem* 2015; **290**: 9767-9779 [PMID: 25713142 DOI: 10.1074/jbc.M115.640656]

43 **Fosnes GS**, Lydersen S, Farup PG. Constipation and diarrhoea - common adverse drug reactions? A cross sectional study in the general population. *BMC Clin Pharmacol* 2011; **11**: 2 [PMID: 21332973 DOI: 10.1186/1472-6904-11-2]

44 **Mosli M**, Parfitt J, Gregor J. Retrospective analysis of disease association and outcome in histologically confirmed ischemic colitis. *J Dig Dis* 2013; **14**: 238-243 [PMID: 23419044 DOI: 10.1111/1751-2980.12045]

P- Reviewer: Koh TW, Wang YN
S- Editor: Ji FF **L- Editor**: A **E- Editor**: Jiao XK

Published by **Baishideng Publishing Group Inc**
8226 Regency Drive, Pleasanton, CA 94588, USA
Telephone: +1-925-223-8242
Fax: +1-925-223-8243
E-mail: bpgoffice@wjgnet.com
Help Desk: http://www.wjgnet.com/esps/helpdesk.aspx
http://www.wjgnet.com